Self-trapped hydrogen states in metals determined from quantum mechanical calculations using potentials based on ab initio data: I. Hydrogen isotopes in Pd

1994 J. Phys.: Condens. Matter 6 7679

(http://iopscience.iop.org/0953-8984/6/38/008)

J. Phys.: Condens. Matter 6 (1994) 7679–7704. Printed in the UK

Self-trapped hydrogen states in metals determined from quantum mechanical calculations using potentials based on *ab initio* data: I. Hydrogen isotopes in Pd

H Krimmel, L Schimmele, C Elsässer and M Fähnle

Institut für Physik, Max-Planck-Institut für Metallforschung, Heisenbergstraße 1, D-70569 Stuttgart, Federal Republic of Germany

Received 15 September 1993, in final form 28 April 1994

Abstract. *Ab initio* pseudopotential calculations for H in Pd are used in order to construct an auxiliary short-ranged host-lattice–particle potential which well reproduces the large number of available *ab initio* data. This potential (instead of an empirical potential as employed in previous treatments) is used in a quantum mechanical calculation of hydrogen as well as of μ^+ and π^+ states in Pd, which takes into account the dependence of the lattice relaxation on particle mass and particle state. These calculations allow us to determine Jahn–Teller coupling constants of excited states and the dependence of lattice displacements on the isotopic mass. It is found that coupling to lattice modes with E-symmetry is dominant. The effect of lattice relaxation on the total energy difference if hydrogen is localized at tetrahedral or octahedral sites and on the excitation energies as measured by inelastic neutron scattering experiments is also discussed.

1. Introduction

The theoretical investigation of the behaviour of a light particle endowed with one positive elementary charge (μ^+, π^+, p, d, t) in a metal is confronted with a complicated many-body problem. The constituents of this many-body system are the particle, i.e. the hydrogen nucleus or $\mu^+(\pi^+)$, the host metal electrons, and the host ions, which are all coupled. Firstly, the system of the host metal electrons is strongly perturbed due to the presence of the particle, giving rise to screening of the particle charge and to modifications in the interactions between the screened host ions. Secondly, the screened particle couples to the host ions which leads to strong local lattice distortions and thus to self-trapping. A further complication comes into the problem because the particle is light and therefore its degrees of freedom have to be treated quantum mechanically. All these effects have to be incorporated into a satisfactory theoretical treatment of the problem.

The phenomena which we want to discuss are energetics and site assignment, lattice displacements in the self-trapped state, local vibrations of the impurity, and diffusion-related properties. The emphasis is on the first three problems whose solution provides the basis for a treatment of the numerous questions related to the field of quantum diffusion. In particular, we want to investigate the dependence of site occupation and of the local lattice distortions on the particle mass. Furthermore, we want to know how big the differences in the lattice distortions are between the particle being in the ground or an excited vibrational state.

The problems mentioned above have already been tackled in several previous treatments on the basis of a computational scheme in which the metal–particle interaction is either

0953-8984/94/387679+26$19.50

described by empirical pair potentials (Sugimoto and Fukai 1980 and 1981, Klamt and Teichler 1986a, 1986b, Christodoulos and Gillan 1991) or within the framework of the quasi-atom (effective medium) theory (Puska and Nieminen 1984). The elastic response of the lattice was described by static lattice Green functions (Sugimoto and Fukai 1980 and 1981, Klamt and Teichler 1986a, 1986b, Puska and Nieminen 1984) and the interactions among the host atoms were modelled by Finnis–Sinclair potentials (Christodoulos and Gillan 1991). The strength of these treatments is that they take the quantum character of the particle fully into account. Their weakness is the use of empirical pair potentials which are obtained by fitting to only a few experimental data, i.e. to typically two or three excitation energies of localized particle vibrations, as determined by inelastic neutron scattering, and to the elastic double-force tensor. First of all this reduces the predictive power of the method and secondly one cannot expect that a detailed and precise modelling of the particle–host interaction is possible in this way. Furthermore, for many materials of interest the required experimental data are not available. In their work Puska and Nieminen (1984) avoided using experimental data. However, because of the use of the quasi-atom concept, quantitative accuracy in the interaction energies could be claimed only at the level of about 0.2–0.5 eV. A treatment based on the quasi-atom concept in its present development is therefore not suited for giving reliable answers to the subtle problems mentioned above.

On the other hand, full *ab initio* computations which include all the different aspects discussed at the beginning of this section are at present, even within the local-density approximation, completely impossible. Therefore a pair-potential description of the particle–host interaction has also been chosen in the present work, but with the important modification that the pair potentials are constructed on the basis of *ab initio* calculations in the local-density approximation. The response of the host lattice is treated using lattice Green functions. In constructing the pair potentials the following data obtained by *ab initio* pseudopotential calculations in the local-density approximation have been used:

(i) total energy curves of ordered metal–hydrogen alloys as a function of the displacement of the hydrogen sublattice relative to the sublattice formed by the host metal;

(ii) forces exerted on neighbouring metal atoms as hydrogen is introduced into the rigid host lattice;

(iii) information on forces contained in the calculated volume expansion due to hydrogen loading.

In the *ab initio* calculations the extension of the hydrogen nuclear wavefunction is entirely neglected. Furthermore, the calculation of the local lattice relaxation is quite time consuming and therefore can be performed for only a few high-symmetry situations. Proceeding in two steps, as will be done in the present work, avoids these shortcomings of state-of-the-art *ab initio* treatments of hydrogen in metals without losing too much of the precision reached by these techniques during the last few years.

The particular material investigated in this part of the present work (part I) is the FCC metal Pd. Part II (Krimmel *et al* 1994) is devoted to α-Fe which crystallizes in the BCC structure. To the best knowledge of the authors the only work that treats particle wavefunction and local lattice relaxation for a FCC metal in detail is the work by Puska and Nieminen (1984) who calculated the ground-state vibrations and the corresponding lattice distortions for various hydrogen 'isotopes' including μ^+ in several FCC metals and at octahedral (O) as well as tetrahedral (T) sites in order to determine the stable site. Earlier work by Teichler (1978) on Cu includes the ground-state wavefunction of the particle in the calculation of lattice relaxations, but not self-consistently, and in very recent calculations of H in Pd with the effective-medium theory (e.g. Christensen *et al* 1990, Engberg *et al* 1993)

the particle is considered as point-like. The aims of the present calculations are as follows.

(i) To determine the sites at which self-localization of the particle takes place and to investigate whether in addition to the self-trapped state with minimum energy there exists a second metastable self-trapped state localized at some other site, the metastable site. The particle-mass dependence of the site-stability will be taken into account.

(ii) To investigate the dependence of the local lattice relaxation at fixed particle mass on the vibrational state of the particle. Particular emphasis is laid on the role of the Jahn–Teller effect of degenerate excited particle states and on the determination of the relevant coupling parameters to the lattice because certain peculiarities in the inelastic neutron scattering spectra in PdH_x were attributed to the Jahn–Teller effect (Klamt 1987).

The layout of the paper is as follows. In section 2 a general outline of the method is given and the basic formulae, although already given in previous papers, are collected and discussed in the context of the present treatment. Section 3 gives details of the construction of the pair potential. Sections 4 to 7 contain the results.

2. The model

The calculation scheme used in the present treatment is the same as the one already employed in a series of previous treatments of hydrogen–metal systems (Sugimoto and Fukai 1980, 1981, Puska and Nieminen 1984, Klamt and Teichler 1986a, 1986b). A modified version of the treatment of the host-atom–host-atom interaction was employed in the work of Christodoulos and Gillan (1991). In order to derive the basic equations, the electronic degrees of freedom are eliminated via the Born–Oppenheimer approximation in a first step. After that the Hamiltonian describing the system consisting now of the host lattice and of the particle coupled to the host-lattice atoms may be written in the form

$$H = T_L + T_P + H^0_{LL}(\boldsymbol{R}) + U(\boldsymbol{R}, \boldsymbol{r}) \tag{1}$$

where T_L and T_P are the kinetic energy operators of the lattice or the particle, respectively, and where the adiabatic potential has been decomposed into a term H^0_{LL} describing the interaction among the lattice atoms in the absence of the particle and a term U which contains all interactions associated with the presence of the particle. $\boldsymbol{R}$ denotes the $3N$ coordinates of the host-lattice atoms and $\boldsymbol{r}$ the particle coordinates. The interaction U may be built up by pairwise interactions between the particle and the neighbouring host-lattice atoms, by the differences in the interaction among host-lattice atoms in the vicinity of the particle which are induced by the particle, and by further many-body effects.

The next step is the adiabatic decoupling of the motion of the particle from that of the host-lattice atoms in a second Born–Oppenheimer approximation. This leads us to the Schrödinger equation

$$[T_P + U(\boldsymbol{R}, \boldsymbol{r})]\psi^\alpha(\boldsymbol{r}, \boldsymbol{R}) = E^\alpha(\boldsymbol{R})\psi^\alpha(\boldsymbol{r}, \boldsymbol{R}) \tag{2}$$

from which the particle wavefunction $\psi^\alpha(\boldsymbol{r}, \boldsymbol{R})$ and energy $E^\alpha(\boldsymbol{R})$ at a fixed configuration of the host lattice may be calculated. In the present treatment the harmonic approximation for the host-lattice interaction H^0_{LL} in the absence of the particle is adopted, i.e.

$$H^0_{LL} = \tfrac{1}{2}\boldsymbol{u}\boldsymbol{D}^0\boldsymbol{u} \tag{3}$$

where $\boldsymbol{u}$ is a $3N$-dimensional vector containing the displacements of the host-lattice atoms from their equilibrium positions ($\boldsymbol{R}^0$) in the lattice without a particle and $\boldsymbol{D}^0$ is the matrix

of force constants of the unloaded lattice. The static equilibrium configuration R^{α}_{eq} or u^{α}_{eq} of the lattice in the presence of the particle in state α is determined by

$$D^0 u^{\alpha}_{eq} + \nabla_u E^{\alpha}(u^{\alpha}_{eq}) = 0 \tag{4}$$

which may be expressed via the Hellmann–Feynman theorem (Hellmann 1937, Feynman 1939) as

$$D^0 u^{\alpha}_{eq} + \langle \psi^{\alpha}(r, u^{\alpha}_{eq}) | \nabla_u U(R^0 + u^{\alpha}_{eq}, r) | \psi^{\alpha}(r, u^{\alpha}_{eq}) \rangle = 0. \tag{5}$$

Equation (5) may then be written in the form

$$u^{\alpha}_{eq} = G^0 F^{\alpha}(u^{\alpha}_{eq}) \tag{6a}$$

$$G^0 := (D^0)^{-1} \tag{6b}$$

$$F^{\alpha}(u) = -\langle \psi^{\alpha}(r, u) | \nabla_u U(R^0 + u, r) | \psi^{\alpha}(r, u) \rangle. \tag{6c}$$

G^0 is the static lattice Green function (Tewary 1973, Leibfried and Breuer 1978) and $F^{\alpha}(u)$ is the expectation value of the forces exerted on the host-lattice atoms at the lattice configuration u, calculated with the eigenfunction of the particle in state α at the same u. If $U(R^0 + u, r)$ and G^0 are known, equations (2), (6*a*) and (6*c*) may be evaluated iteratively in the way described by Sugimoto and Fukai (1980, 1981), Puska and Nieminen (1984), and by Klamt and Teichler (1986a, 1986b) in order to obtain self-consistent solutions, i.e. the equilibrium displacements u^{α}_{eq} which are consistent with the forces calculated from (6*a*) and (6*c*) using the solution $\psi^{\alpha}(r, u_{eq})$ of the Schrödinger equation (2) in the potential which corresponds to the displacements u_{eq}.

In order to illustrate some general problems we first describe the potential surface $U(R^0 + u, r)$ approximately as a sum of pair potentials $\tilde{V}$ between the particle and the host atoms and by an additional term which takes into account that the force constants between the host atoms in the vicinity of the particle may be different from those in the unloaded lattice. This change in the force-constant matrix is denoted by δD. Thus one obtains

$$U(R^0 + u, r) = \sum_n \tilde{V}(r - (R^0_n + u_n)) + \tfrac{1}{2} u \delta D(r) u \tag{7}$$

where R^0_n, u_n are now three-component vectors giving the position of the host atom with number n. From (6*c*) one obtains

$$F^{\alpha}(u, r) = -\sum_n \langle \psi^{\alpha} | \nabla_{u_n} \tilde{V}(r - (R^0_n + u_n)) | \psi^{\alpha} \rangle - \langle \psi^{\alpha} | \delta D | \psi^{\alpha} \rangle u. \tag{8}$$

The first term in (8) is non-vanishing for $u_n = 0$. Each term in the sum over n contributes to just the components of F^{α} describing the forces on atom n. Of course, the first term in (8) could be replaced or supplemented by more complicated many-body forces. The second term is non-vanishing only for $u \neq 0$. Although this term should be better viewed as contributing to the elastic energy of the host lattice, it is attributed to the particle energy. If in the following we speak of an elastic energy, we are referring only to the elastic energy that is stored in the unloaded reference lattice if the same lattice displacements are introduced there as in the lattice containing the particle. This energy is given by

$$E_{el} = \tfrac{1}{2} u D^0 u = \tfrac{1}{2} F u. \tag{9}$$

Now we can formulate the requirements for an adequate treatment of the particle–host system. Firstly, we have to demand that the r dependence of $U(R, r)$ is modelled precisely enough for all relevant lattice configurations R and those values of r which are important in order to calculate accurate particle wavefunctions and vibrational energies (measured from the minimum of $U(R, r)$ as a function of r). Secondly, we have to know those terms which

do not greatly change the shape of $U(\boldsymbol{R}, \boldsymbol{r})$ as a function of $\boldsymbol{r}$ but lead to a shift of the potential as $\boldsymbol{R}$ is changed from $\boldsymbol{R}^0$ to $\boldsymbol{R}^0+\boldsymbol{u}$. One term of this kind is the second one in (8) since $\delta \boldsymbol{D}(\boldsymbol{r})$ presumably depends only weakly on $\boldsymbol{r}$. This term has a quadratic dependence on $\boldsymbol{u}$. However, contributions to $U(\boldsymbol{R}, \boldsymbol{r})$ depending weakly on $\boldsymbol{r}$ and contributing already to linear order in $\boldsymbol{u}$ are conceivable as well. Such terms are important for two reasons: firstly, they may enter into the total energetics which, for example, becomes relevant if the relative stability of different sites occupied by the particle is investigated; secondly, they enter into the fictitious forces which act on the reference lattice. In this way these terms affect the determination of $\boldsymbol{u}_{\mathrm{eq}}$ and of the elastic energy.

In the following we describe all the discussed effects approximately by a superposition of radial pair potentials

$$U(\boldsymbol{R}, \boldsymbol{r}) = \sum_n V(|\boldsymbol{r} - \boldsymbol{R}_n|). \tag{10}$$

At first sight the individual terms in (10) seem to be unsuited to describing the contribution of the elastic energy $\frac{1}{2}\boldsymbol{u}\delta\boldsymbol{D}\boldsymbol{u}$ to $U(\boldsymbol{R}, \boldsymbol{r})$, because each individual interaction in (10) gives rise to forces on the particle and on the host atoms which are related by the principle of action and reaction whereas $\frac{1}{2}\boldsymbol{u}\delta\boldsymbol{D}\boldsymbol{u}$ leads to forces on the host atoms (for $\boldsymbol{u} \neq 0$), but not necessarily to forces on the particle. However, due to the occurrence of the sum over host lattice atoms the *ansatz* is flexible enough to describe approximately all the various effects discussed before.

In order to determine the parameters which appear in V, the *ansatz* (10) was fitted to the following data, which for the main part are results of self-consistent *ab initio* pseudopotential calculations (Elsässer 1990, Elsässer *et al* 1991a, 1991b, 1992, 1994a, 1994b) based on the density functional theory in the local-density approximation:

(i) a whole set of energy versus displacement curves which were obtained in a series of total energy calculations for a supercell geometry in which the hydrogen sublattice was rigidly displaced relative to the host lattice along certain high-symmetry directions; thereby the local relaxation of the host-lattice atoms surrounding the particles is not considered, but a volume expansion of the supercells due to the introduction of the particles is taken into account;

(ii) forces that act on neighbouring host-lattice atoms if a hydrogen atom is placed at some high-symmetry position and the lattice atoms are kept at the sites of the unloaded lattice;

(iii) the elastic double-force tensor determined from either the measured or the calculated volume expansion caused by loading the host crystal with hydrogen.

A detailed discussion of the particular data used in order to construct pair potentials is given separately in section 3 for Pd and in section 2 of part II (Krimmel *et al* 1994) for Fe. However, a few general remarks will be given here.

The energy versus displacement curves at a given lattice configuration $\boldsymbol{R}$ (undistorted host lattice with the new equilibrium lattice constant for the loaded system) are only available for materials with a high hydrogen content (PdH, Pd_4H, FeH) because only in such cases can one work with supercells that are small enough to keep the computing effort within reasonable bounds. On the other hand, our ultimate aim is the investigation of the properties of a single defect (limit of low defect concentration) and not of a dense defect lattice. In the case of Pd where energy versus displacement curves are available for more than one single hydrogen concentration, it is therefore tempting to give higher priority to a good fit of the pair potential to the energy curves of the material with lower hydrogen content (see below). Nevertheless, the other energy curve is also included in the fitting procedure

because we can expect that this will improve the transferability with regard to changes in the host-atom distances. In fact, the energy versus displacement curves were calculated at the equilibrium lattice constant which changes with hydrogen content. On the other hand, one might think that the variation of the hydrogen content leads to additional variations in the pair and many-body interactions which are not describable in terms of a dependence on the lattice constant (or lattice configuration $\boldsymbol{R}$). Since we are only interested in the low-concentration limit we would not want this dependence to be included. However, such effects appear to be unimportant. We note that the pair interactions among the hydrogen atoms do not influence the shape of the energy versus displacement curves but lead only to a constant energy shift because the hydrogen sublattice is shifted rigidly relative to the host lattice. The same is apparently true for other interactions since calculations of the energy differences between the octahedral and the tetrahedral site as well as between the octahedral site and the lowest lying saddle point performed on PdH_x *at fixed lattice constant* and for hydrogen concentrations ranging from $x = 1$ to $x = 1/32$ show that these energy differences are essentially independent of the hydrogen content. Therefore, the changes in the energy versus displacement curves, calculated at the equilibrium lattice constant, as one goes from PdH to Pd_4H should reflect the variation of the potential energy surface $U(\boldsymbol{R}, \boldsymbol{r})$ with the lattice configuration $\boldsymbol{R}$ for a single hydrogen atom in the host crystal. From this point of view the energy curves which should get the largest weight in the fitting procedure are those corresponding to nearest-neighbour distances which are near to the typical host-atom–host-atom distances in the locally relaxed environment of the hydrogen impurity. For hydrogen placed at an O site this is the case for Pd_4H as shown below.

The fit of (10) to the energy versus displacement curves is not unique. Many very different pair potentials (purely repulsive potentials as well as potentials which are attractive at larger distances) give very good fits. This freedom can be used and has to be used to incorporate information on forces into the pair potential. The *ab initio* computation of forces representative for a single hydrogen atom requires the use of rather large supercells since the computed forces are the result of the superposition of the individual contributions from all hydrogen atoms of the hydrogen sublattice and are therefore largely determined by symmetry conditions for small supercells. For hydrogen sitting at high-symmetry sites and for small supercells the forces on neighbouring atoms are bound to vanish. Of particular importance is the knowledge of the forces acting on the neighbouring host atoms of hydrogen placed at a local minimum or at a saddle point of $U(\boldsymbol{R}^0, \boldsymbol{r})$. The local minima are important because there the occupation probability for the particle may have maxima and therefore these points are representative for the computation of the forces $\boldsymbol{F}^\alpha$ from equation (6*c*). The forces on the neighbouring host atoms of a particle at a saddle point may become important in the calculation of transport properties (of saddle-point energies, for instance), or in some cases it may even happen that a saddle point is converted into a local minimum due to lattice relaxations. Additional information on the forces at the stationary points is also needed because, even if only pair interactions are relevant, the energy versus displacement curves give the least reliable information on forces between an individual pair of atoms for a particle located in the vicinity of such points. The contribution to the forces due to the change $\delta \boldsymbol{D}$ in the force-constant matrix are not included in the *ab initio* forces since these are calculated neglecting local lattice relaxation. However, many-body effects contributing to $U(\boldsymbol{R}, \boldsymbol{r})$ and to linear order in $\boldsymbol{u}$ are included in the *ab initio* forces.

Information on the '$\delta \boldsymbol{D}$ terms' is, however, included in the double-force tensor which is defined by

$$P_{ij} = \sum_n R_i^0(n) F_j(n) \tag{11}$$

where $F_j(n)$ is the jth component of the force (6c) on the nth host atom and $R_i^0(n)$ the i component of its distance vector from the particle. The trace of $\boldsymbol{P}$ may be determined from the volume change per hydrogen impurity of the host crystal, which may be either derived from *ab initio* calculations or, if available, from experiment. Very recently the components of $\boldsymbol{P}$ have been calculated *ab initio* directly from the Hellmann–Feynman forces on Pd and Nb atoms in a series of cubic supercells (Elsässer *et al* 1994b). The experimentally measured volume change for cubic symmetry is given by (see, e.g., Leibfried and Breuer 1978, Peisl 1978)

$$\Delta V = \mathrm{tr}P/(3K) \tag{12}$$

where K is the bulk modulus. In the *ab initio* calculation the situation corresponds to a particle with a δ-shaped wavefunction placed at some interstitial site and therefore in calculating the forces which appear in (11) no quantum mechanical averaging has to be considered. In contrast, the experimental value of P_{ij} is determined by the quantum mechanical expectation value of the forces and hence is related to the real wavefunction of the particle. From the double-force tensor, information about forces acting on particular neighbouring host atoms can be determined only if the particle occupies high-symmetry sites and if the pair interactions are of short range otherwise the number of unknown forces exceeds by far the number of independent equations provided by $\boldsymbol{P}$. In the following, the interactions will be cut off by a smooth cut-off function such that the forces are non-vanishing only for the host atoms in the first- and second-neighbour shell of an O or T site.

Table 1. *Ab initio* forces on the nearest-neighbour atoms in units of eV Å^{-1} for hydrogen on the tetrahedral (T), octahedral (O), and the triangular saddle point S_{111} (see figure 1). Pd atoms on regular lattice positions, lattice constant $a = 3.88$ Å. Uncorrected data in round brackets (see text).

	H on T site	H on S_{111}	H on O site
$Pd_{32}H$	(1.54) 1.77	(2.47) 2.70	(0.05) 0.23
$Pd_{16}H$	(1.59) 1.70	(2.44) 2.57	(0.15) 0.26
Pd_8H	(1.62) 1.70	(2.65) 2.57	(0.31) 0.33

3. Determination of the pair potential

In constructing the pair potential data obtained by *ab initio* pseudopotential calculations (Elsässer 1990, Elsässer *et al* 1991a, 1991b, 1992, 1994b) on cubic Pd_nH supercells ($n = 1, 4, 8, 16, 32$) are used following the general principles outlined in section 2. Energy versus displacement curves are available for PdH supercells at the *ab initio* equilibrium lattice constant $a = 4.07$ Å, for H placed at the octahedral site, and for Pd_4H ($a = 3.94$ Å) (see Elsässer 1990, Elsässer *et al* 1991a, 1991b, 1992). For comparison, the *ab initio* lattice constant for unloaded Pd is $a = 3.88$ Å. The energy versus displacement curves were calculated along the four directions depicted in figure 1 by computing the total energies as the hydrogen atom in the respective supercell is placed at a series of different points on these lines while the Pd atoms are held fixed at the positions they take if hydrogen sits at O sites. The energy of the system if H is at an O site was chosen as energy zero. These data are shown as crosses in figures 2 and 3. Forces acting on Pd atoms in the neighbourhood of hydrogen were calculated by Elsässer *et al* (1992, 1994b) using the

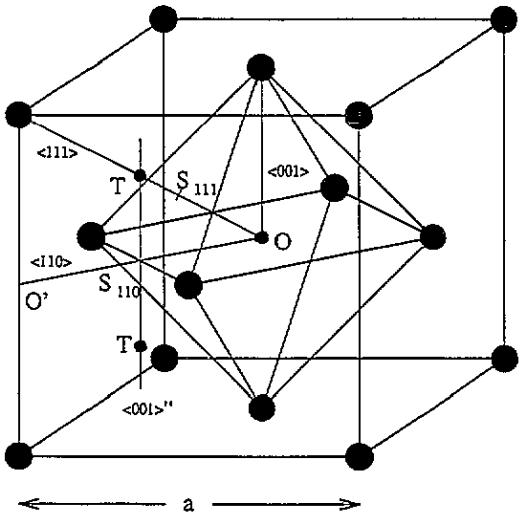

Figure 1. The elementary unit cell of face-centred cubic Pd with the lines along which the energy versus displacement curves have been calculated *ab initio*.

Hellmann–Feynman theorem. Forces which are useful for our purposes may be obtained only for larger supercells, i.e. Pd_8H, $Pd_{16}H$, $Pd_{32}H$. All forces were calculated for the Pd atoms held fixed at the positions of an unloaded Pd lattice. Forces which act on the nearest-neighbour atoms if hydrogen sits at an octahedral (O) site, on a tetrahedral (T) site or at the triangular saddle point S_{111} (see figure 1) are given in table 1. The values in round brackets are the ones calculated by Elsässer *et al* (1992). The other data were obtained by Elsässer *et al* (1994b) after submission of the present paper. Both data sets are based on the same computational results, however, an improved analysis as developed by Elsässer *et al* (1994a, 1994c) has been employed in the recent paper by Elsässer *et al* (1994b). The absolute differences in the two data sets are small and are significant therefore only in the case where the forces are small anyway. This happens to be the case for the forces acting on the nearest neighbours of hydrogen placed at an O site as well as for the forces on second and further distant neighbours if hydrogen is placed at either a T site, the saddle point S_{111}, or an O site (forces on second and further distant neighbours may be found in Elsässer *et al* 1994b). A comparison of the results obtained for different supercell sizes (different hydrogen–hydrogen distances) shows that for both data sets the forces acting on the nearest neighbours of H at T or S_{111} are converged with respect to the supercell size (see table 1). Apparently, this is not true for forces exerted on the nearest-neighbour Pd atoms of hydrogen placed at the O site if these are calculated according to the old scheme (in table 1 the data in round brackets). The convergence with respect to the supercell size, however, is considerably improved for the corrected data. This together with the findings that in the $Pd_{32}H$ supercell calculation the corrected forces on the atoms in the second-neighbour shell of the O site are positive (repulsive) and that the double-force tensor comes out positive and with a reasonable magnitude (see Elsässer *et al* 1994b and comments below), in contrast to an unphysical negative double-force tensor obtained from the uncorrected forces for hydrogen on O sites, gives us the confidence that the corrected forces on the nearest as well as on the second nearest neighbours of hydrogen on O sites may be used in the construction of the pair potential. The forces on atoms in the third and fourth neighbour shell of the O site come out very small and negative (attractive) but are well below the

estimated confidence level of about 0.1 eV $Å^{-1}$ and for $Pd_{32}H$ may even still be affected by the superposition of force patterns due to hydrogen in neighbouring supercells. The situation is similar for the more distant Pd shells of hydrogen at T or S_{111}. In view of the lack of trustworthy information on forces at larger distances we have chosen to cut off the pair potential at distances between the second- and third-neighbour shell of the O site. It should be noted, however, that the trace of the double-force tensor computed for hydrogen at O sites from the corrected forces on the first and second Pd shell (neglecting further distant shells) is only about 7.0 eV and thus smaller than the experimental value $\mathrm{tr}\boldsymbol{P} = 10.0 \pm 0.5$ eV (see Peisl 1978) and smaller than the values obtained from the lattice-parameter change upon hydrogen loading as determined from the *ab initio* calculations on the Pd_nH supercells. Linear extrapolation of the Pd_nH data to small hydrogen concentrations gives $\mathrm{tr}\boldsymbol{P} = 9.0$eV, (PdH) or $\mathrm{tr}\boldsymbol{P} = 11.0$ eV (Pd_4H). This discrepancy may have its origin either in a longer range of the forces or in an underestimation of the forces on the two closest Pd shells. In the following we give results obtained with two different pair potentials. Pair potential I is the one which was constructed before the corrected force values were available, pair potential II is the one which incorporates these corrected forces. Both pair potentials give a very good description of the energy versus displacement curves over most hydrogen positions for which *ab initio* data are available. At lower energies differences in this respect exist only in details except for the ⟨111⟩ direction connecting the O and the T site. For this direction, as discussed in length below, the overall performance of pair potential II is better. On the other hand the energy range covered by pair potential I is larger. Furthermore, both potentials describe the forces on the nearest neighbours if hydrogen is placed at the T site or at the triangular saddle point S_{111} almost equally well (pair potential I reproduces perfectly the data in round brackets, pair potential II the corrected data in table 1, which are quite close to the uncorrected ones). However, pair potential II presumably gives a better description of the forces at distances corresponding to the nearest- and second-neighbour shell of the O site because it is fitted to the *ab initio* forces acting on the atoms of these shells. In contrast, in constructing pair potential I no corresponding *ab initio* forces had been used since we did not trust the uncorrected *ab initio* forces on these atoms available at that time, and this turned out to be wise. Information on these forces was included only in so far as a reasonable description of $\mathrm{tr}\boldsymbol{P}$ for hydrogen at an O site was demanded (a detailed comparison of *ab initio* forces and forces calculated from the two pair potentials is given below). However, fixing the value of $\mathrm{tr}\boldsymbol{P}$ even if short-range forces are assumed still leaves freedom in 'distributing the forces' among the two neighbouring shells.

In our judgement, pair potential II is the one which is much better and should be used if, as in the present paper, equilibrium properties are to be calculated. We give, nevertheless, pair potential I since it may be useful for other purposes. We also include the data obtained with pair potential I in tables 2–9 (data in round brackets) because a comparison of the two data sets shows which of the results might be sensitive to some remaining uncertainties existing at the present stage of development of the method and since it indicates how big the resulting uncertainties in the results might be.

The explicit analytical expressions for the two pair potentials determined by this procedure are as follows. Pair potential I is given by

$$\begin{aligned} V^{\mathrm{I}}(r)/eV = {} & 1363.4673\exp(-r/0.04582a) + 1.5716\exp[-(r/a)^{5.6154}/0.001982] \\ & +\{0.3033[\exp((r-0.6147a)/0.07184a)+1]^{-1} \\ & +2.2055\exp(-r/0.24727a)\}f(r) \end{aligned} \tag{13}$$

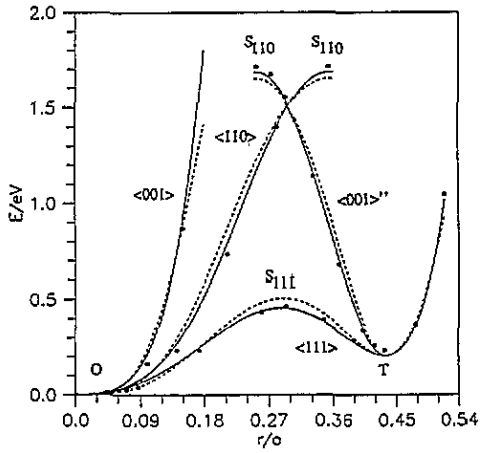

Figure 2. The pair-potential description of the *ab initio* calculated energy versus displacement curves (crosses) of Pd_4H ($a = 3.94$ Å) along the various paths given in figure 1. Solid curves correspond to pair potential I, dashed curves to pair potential II.

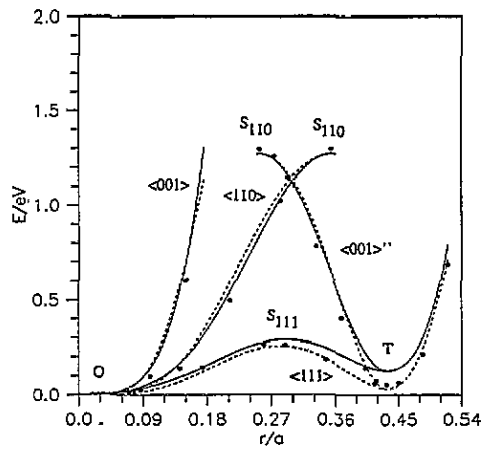

Figure 3. The pair-potential description of the *ab initio* calculated energy versus displacement (crosses) for PdH ($a = 4.07$ Å) along the paths shown in figure 1. Solid curves correspond to pair potential I, dashed curves to pair potential II.

with the smooth cut-off function (Klamt and Teichler 1986a, 1986b)

$$f(r) = \begin{cases} \exp[-r^2/(a^2 - r^2)] & \text{for } r < a \\ 0 & \text{for } r \geqslant a \end{cases} \tag{14}$$

($a = 3.94$ Å is the lattice constant of Pd_4H) for the long-range part of the potential introduced in order to avoid artefacts due to abruptly cutting off the potential).

Pair potential II is parametrized by the following simple expression:

$$V^{II}(r)/eV = \{3.9598 \exp[-(r/a)^{5.9032}/0.002075] + 0.74295\} g(r) \tag{15}$$

with

$$g(r) = \begin{cases} 1 - \exp[-(r-a)^2/(0.6633a)^2] & \text{for } r \leqslant a \\ 0 & \text{for } r > a \end{cases} \tag{16}$$

($a = 3.94$ Å). At large distances the behaviour of $V^{II}(r)$ is determined by $g(r)$ which at the same time serves as a cut-off function.

The energy versus displacement curves computed from the two pair potentials at the lattice constant of Pd_4H are shown in figure 2 (the solid curves correspond to pair potential I, the dashed curves to pair potential II) together with the *ab initio* data for Pd_4H. The analogous curves obtained at the PdH lattice constant are given in figure 3 together with the PdH *ab initio* data. Both pair potentials give a remarkably good overall description of the energy versus displacement curves for Pd_4H as well as for PdH. A big difference between the calculations performed with pair potentials I and II occurs if hydrogen is shifted along the ⟨001⟩ direction from the O site towards a nearest-neighbour Pd atom. The *ab initio* results at $r/a = 0.2$ from the O site along this direction are $E \approx 3.1$ eV (Pd_4H) or $E \approx 2.4$ eV (PdH) (these data are omitted in figures 2 and 3 because they lie outside the energy scale of these figures) and are in very good agreement with the energy values calculated from pair potential I whereas pair potential II gives far too small energies at this hydrogen position. This means that pair potential II is too soft at short distances. Such high energies, however, are not relevant to the calculation of equilibrium properties as performed in the present paper, but may become important in molecular dynamics simulations.

Pair potential I gives a good fit to the *ab initio* energy versus displacement curves obtained for Pd_4H whereas the curves calculated with pair potential II deviate slightly more. This statement is still correct for the PdH curves with the exception of the curve along the ⟨111⟩ direction which starts at the O site, passes first through S_{111} and then through the tetrahedral site. Nevertheless, pair potential II gives a good enough fit even to the Pd_4H energy curves so that a high-quality description of hydrogen vibrational energies and wavefunctions can be expected even for situations in which the distances between hydrogen and the nearest-neighbour Pd atoms after lattice relaxation are in better correspondence to the Pd_4H than to the PdH lattice constant. This is particularly so if states localized near the O site are considered. The advantage of pair potential II is that it gives a very reasonable description of the energy versus displacement curve along ⟨111⟩ for PdH as well as for Pd_4H whereas pair potential I gives a less satisfactory description for PdH. According to our remarks in section 2 this is equivalent to a good representation of the energy versus displacement curves of isolated hydrogen in a rigid lattice and at two lattice constants, i.e. 4.07 Å (PdH) and 3.94 Å (Pd_4H). The same seems to be true at the Pd lattice constant (3.88 Å) where the full energy versus displacement curve is not known but the energy difference between the local minima at T and O sites as obtained from *ab initio* computations is well reproduced by pair potential II. The good description by pair potential II of the minimum at T sites for several lattice constants indicates that the sharp bend in pair potential II (see figure 4) just above the distance between the T sites and its nearest Pd neighbours (at the Pd lattice constant) is real (see also section 6).

A further advantage of pair potential II is that in its construction *ab initio* forces at distances corresponding to the nearest and next-nearest Pd shells of an O site are explicitly used. For this reason it is expected that the local lattice relaxation of states concentrated around the O site is better described by pair potential II. In order to give a comparison of the two pair potentials in this respect we list the values of the forces on the first and second Pd shell due to hydrogen at an O site and of $\mathrm{tr}P$ as calculated from both pair potentials together with the corresponding *ab initio* data. The forces on the atoms in the first shell are 0.66 eV Å^{-1} (pair potential I), 0.27 eV (pair potential II), 0.23 eV Å^{-1} (*ab initio*); the forces on the second shell 0.04 eV Å^{-1} (pair potential I), 0.12 eV Å^{-1} (pair potential II), 0.15 eV Å^{-1} (*ab initio*). $\mathrm{Tr}P$ is 8.8 eV (pair potential I, 9.1 eV for protons if the extension of the wavefunction is included), 6.4 eV (pair potential II, 7.3 eV for P), 7.0 eV (*ab initio*

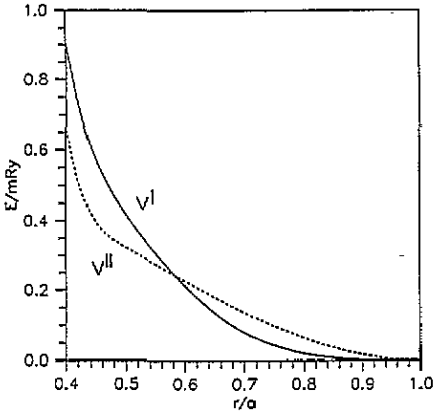

Figure 4. Pair potential I and II.

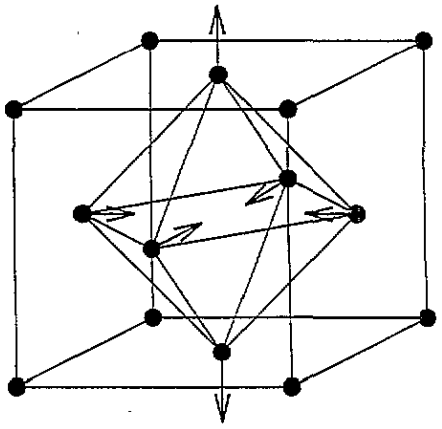

Figure 5. Example of a tetragonal distortion according to E-mode coupling.

if only two shells are included). Since pair potential II gives forces which decay only very slowly between the first and the second Pd shell, the behaviour of pair potential II is less smooth than that of pair potential I (see figure 4), but as mentioned above, additional support for this type of distance dependence of $V^{II}(r)$ comes from the energy curves along ⟨111⟩. It is clear that the displacements of the nearest neighbours which are obtained if pair potential II is employed will be smaller than the corresponding values obtained with pair potential I. This will also lead to smaller elastic energies if the calculations are performed with pair potential II. On the other hand, these elastic energies are somewhat underestimated since pair potential II gives a too small tr$P$. How other quantities such as the vibrational energies or the Jahn–Teller coupling energies are affected by changing from pair potential I to pair potential II remains to be seen.

4. Particle states in the rigid palladium lattice

The particle states in the periodic potential due to the rigid Pd lattice (lattice constant = 3.88 Å) are calculated in order to give a survey over the states and their local symmetries and because they will be needed later as a reference in the calculation of self-trapping energies. The calculations are restricted to the Γ point (reciprocal lattice vector $k = 0$). This is sufficient since the energy bands are extremely narrow. The solution of the Schrödinger equation is accomplished by a method first described by Kimball and Shortley (1934) imposing periodic boundary conditions on the wavefunction. A detailed description is also given in the work of Puska and Nieminen (1984). In order to obtain accurate and stable solutions symmetry arguments should be exploited. Full use of symmetry is absolutely necessary if degenerate or nearly degenerate eigenstates are calculated. The calculations have been performed on a mesh of points building a simple cubic lattice. In order to test the convergence with respect to the number of mesh points, calculations were performed with several mesh widths, in particular with a width of 0.0647 Å and 0.0485 Å. Table 2 gives the energies E_i^P of the six lowest eigenstates which all have the maximum occupation probabilities at the O site, measured from the potential minimum of the periodic potential

at the O site, as well as symmetry (the Mullikan notation is used, see, e.g., Burns 1977) and degeneracy of the states.

Table 2. Eigenstates of the hydrogen isotopes (μ^+, π^+, p, d, t). Symmetry (Mullikan notation), degeneracy, vibrational energies (energies E_i above the potential minimum at the O site, obtained with potential II and, in brackets, with potential I) calculated (1) in the periodic potential of the rigid Pd lattice ($a = 3.88$Å) at the Γ point (E_i^p; all states have the maximum occupation probability at O sites) (2) in the potential corresponding to the lattice configuration of the self-trapped ground state (marked STGS). In all calculations a mesh width of 0.0647 Å has been used. For comparison the *ab initio* results for undistorted Pd_4H at the equilibrium lattice constant $a = 3.94$ Å (Elsässer *et al* 1991b) are given (lines marked with Pd_4H).

	State i	0	1	2	3	4	5
	Symmetry	A_{1g}	T_{1u}	T_{2g}	A_{1g}	E_g	A_{2u}
	Degeneracy	1	3	3	1	2	2
	E_i^p	468 (464)	814 (817)				
μ^+	E_i (meV) (STGS)	409 (390)	722 (686)				
	E_i^p	399 (394)	696 (689)				
π^+	E_i (meV) (STGS)	348 (331)	617 (582)				
	E_i^p	129 (131)	227 (227)	317 (314)	337 (331)	357 (349)	(393)
p	E_i (meV) (STGS)	112 (109)	200 (190)	280 (263)	301 (281)	321 (297)	(329)
	(Pd_4H)	106	189	264	285	303	330
	E_i^p	86 (89)	150 (152)	210 (212)	223 (222)	233 (231)	(267)
d	E_i (meV) (STGS)	74 (73)	132 (127)	185 (177)	198 (187)	209 (195)	(222)
	(Pd_4H)	70	124	174	188	198	220
	E_i^p	67 (71)	118 (121)	165 (169)	175 (175)	182 (181)	(213)
t	E_i (meV) (STGS)	58 (58)	103 (101)	145 (140)	155 (147)	162 (153)	(177)
	(Pd_4H)	55	98	137	148	155	177

The entries in table 2 as well as in all following calculations in sections 5 to 7 of wavefunctions and energies are determined on a grid with mesh width of 0.0647 Å. The ground-state energies calculated with a mesh width of 0.0485 Å are higher by 0.8 meV, 0.6 meV or 0.4 meV for μ^+, π^+ and the 'true' hydrogen isotopes p, d, t. The excitation energies up to the fifth excited state come out by about 1 to 3 meV higher as the mesh width is reduced from 0.0647 to 0.0485 Å. The variation is always larger for the lighter particle and the higher excited state.

The number of iteration steps that have to be performed until the energy eigenvalues at a given mesh width are stationary within given accuracy limits increases rapidly with decreasing mesh width. The accuracy with respect to the number of iteration steps is better than 0.1 meV.

In table 2 the numbers in round brackets are calculated with pair potential I, the others with pair potential II. Differences in the two data sets obtained at the fixed rigid Pd lattice configuration but with two different pair potentials reflect, in the first place, slight differences in the quality of the fits to the *ab initio* adiabatic potentials (in particular to the one obtained for Pd_4H) and, in the second place, a slightly different extrapolation of the adiabatic potential to the Pd lattice constant. These differences, however, are not serious. The energies of the eigenstates below and around 200 meV come out somewhat smaller if the calculations are

carried out with pair potential II because this potential gives rise to a wider bottom of the potential well at the O site than pair potential I, in better agreement with the *ab initio* data (see figures 2 and 3). For higher energy states the situation is reversed. Figure 2 gives an obvious explanation for this reversal.

5. Self-localized states at the octahedral site

In order to investigate self-localized states centred at an O site it is demanded that the wavefunction vanishes on the surface of a sufficiently large sphere surrounding the O site. The wavefunctions and local lattice distortions are calculated iteratively from equations (2), (6*a*) and (6*c*) using the static lattice Green function given by MacGillivray and Sholl (1983). The relaxation of the 14 nearest and next-nearest neighbour Pd atoms is considered. The total energy change with respect to the energy of the corresponding state in the rigid, undeformed lattice, i.e. the self-trapping energy, may be written as

$$\Delta E_i^{\mathrm{tot}} = \Delta E_i^{\mathrm{vib}} + \Delta E_i^{\mathrm{min}} + E_i^{\mathrm{def}}. \tag{17}$$

The first term in (17) is defined as $\Delta E_i^{\mathrm{vib}} = E_i^{\mathrm{st}} - E_i^{\mathrm{p}}$, where E_i^{st} is the vibrational energy measured from the bottom of the local potential minimum formed after self-trapping and E_i^{p} is the corresponding vibrational energy in the periodic potential of the rigid lattice (see table 2). In the following, the superscript 'st' is skipped for notational convenience. In other words, $\Delta E_i^{\mathrm{vib}}$ is the change in the vibrational energy caused by the change of the width of the potential well due to lattice relaxation. $\Delta E_i^{\mathrm{min}}$ is the shift in energy of the bottom of the potential well caused by lattice relaxation, and E_i^{def} is the elastic energy which has to be brought up in order to deform the host lattice. E_i^{def} is calculated from equation (9) using the self-consistently determined forces and displacements. $\Delta E_i^{\mathrm{vib}}$ depends of course on the vibrational state. However, $\Delta E_i^{\mathrm{min}}$ and E_i^{def} may also show some dependence on the vibrational state because the expectation values of forces (see equation (8)) depend somewhat on the particle's vibrational state. Such effects are discussed in section 6. Table 3 shows the ground-state vibrational energies E_0 of various isotopes as well as the self-trapping energies $\Delta E_0^{\mathrm{tot}}$ together with the individual terms of equation (17) contributing to the latter. Furthermore, the displacements of the nearest and next-nearest neighbour Pd atoms in units of the lattice constant $a = 3.88$ Å of the unloaded Pd lattice and the trace of the double-force tensor are given. Table 3 shows that at least for the light isotopes a quite substantial isotope effect exists for all quantities related to the local lattice deformations, which is completely missed in typical *ab initio* methods where for the calculation of lattice relaxations hydrogen is treated as a classical particle (corresponding to a particle with infinite mass). Since pair potential II gives forces on the nearest-neighbour Pd shell which are considerable smaller than those caused by pair potential I, calculations with pair potential II give much smaller displacements of the nearest-neighbour Pd atoms than corresponding ones performed with pair potential I. For this reason all energy changes associated with lattice relaxation are much smaller if they are computed with pair potential II. The larger forces on the second neighbours obtained with pair potential II in comparison with potential I cannot reverse this trend. With respect to the isotope effects the difference between the two data sets is less dramatic. In view of the *ab initio* forces, however, we give a clear preference to the data obtained with pair potential II. Nevertheless, one should be aware of the fact that the too small $\mathrm{tr}\boldsymbol{P}$ indicates that the deformation energy associated with states localized at an O site might be underestimated in the calculations performed with pair potential II. Whether this remaining uncertainty influences $\Delta E_i^{\mathrm{vib}}$ and $\Delta E_i^{\mathrm{min}}$ depends on whether the origin of the discrepancy in $\mathrm{tr}\boldsymbol{P}$ of the O as calculated from the *ab initio* forces or from the volume

expansion (*ab initio* or measured) is mainly due to a longer range of the forces or mainly caused by remaining uncertainties in the short-range forces. Only in the latter case is a significant modification of ΔE_i^{vib} or ΔE_i^{min} expected.

Table 3. Ground-state vibrational energy E_0 in the self-trapped state at an O site in Pd, change of the vibrational energy ΔE_0^{vib} and change of the energy of the bottom of the potential well relative to the rigid lattice ΔE_0^{min}, deformation energy E_0^{def}, total energy gain ΔE_0^{tot} due to self-trapping, relative lattice displacements of the nearest- and next-nearest-neighbour Pd atoms, and trace of the double-force tensor for the various hydrogen isotopes (mesh width 0.0647 Å). The Pd atoms are displaced radially outwards from the O site. The calculations have been performed with pair potentials I and II. Results obtained with pair potential I are given in round brackets.

	E_0	ΔE_0^{vib} (meV)	ΔE_0^{min} (meV)	E_0^{def} (meV)	ΔE_0^{tot} (meV)	$(\Delta l/a)_{\text{NN}}$ (%)	$(\Delta l/a)_{\text{NNN}}$ (%)	$Tr(P)$ (eV)
μ^+	409	−59	−71	62	− 68	0.97	0.34	8.82
	(390)	(−74)	(−229)	(142)	(−162)	(1.54)	(0.09)	(10.55)
π^+	348	−50	− 68	57	−62	0.92	0.35	8.55
	(331)	(−63)	(−224)	(135)	(−153)	(1.50)	(0.09)	(10.29)
p	112	−17	−55	35	−37	0.68	0.37	7.25
	(109)	(−22)	(−199)	(105)	(−115)	(1.32)	(0.09)	(9.14)
d	74	−11	−53	31	−33	0.63	0.38	6.96
	(73)	(−15)	(−194)	(100)	(−109)	(1.29)	(0.09)	(8.92)
t	58	−9	−51	29	−31	0.61	0.38	6.83
	(58)	(−12)	(−192)	(98)	(−106)	(1.27)	(0.09)	(8.82)

5.1. Excited states in the potential of the ground-state configuration

The vibrational energies of excited states which are calculated in the potential corresponding to the lattice configuration of the self-trapped ground state (STGS) are given in table 2 in the lines marked STGS. For comparison we give hydrogen vibrational energies in the *ab initio* adiabatic potential of hydrogen in Pd_4H. A very close agreement between these data and those obtained with pair potential I is found which is due to the fact that the distances of the nearest-neighbour Pd atoms from the O site are almost identical in the relaxed ground-state configuration as determined with pair potential I and in Pd_4H. The changes in the vibrational energies depend on whether pair potential I or II is used. This dependence is less pronounced for the excitation energies $E_i - E_0$ in the fixed ground-state configuration due to a partial cancellation of relaxation effects. The differences between the excitation energies obtained with the two pair potentials are 10% or less. These excitation energies are frequently used in interpretations of inelastic neutron scattering spectra (see, e.g., Christodoulos and Gillan 1991). It is argued that the excitation process is so fast that the lattice does not have the time to respond to the new particle state. However, quantum mechanical calculations show that this picture is only applicable in the case of a strong particle–lattice coupling whereas in the case of weak coupling the zero-phonon line dominates, which corresponds to the difference between the total energy of the excited state in the lattice configuration calculated according to the force expectation value in this state and the ground-state energy (see Klamt 1986, Stoneham 1975 and references therein).

In section 5.2 it will be shown that in the hydrogen–palladium system the weak coupling situation is realized and that therefore the peak positions in the inelastic neutron scattering spectra are not directly given by the excitation energies calculated from the entries in table 2.

The data of table 2 are nevertheless very important in that the differences between the total energies of the excited states in the ground-state configuration and the total energies obtained in calculations in which the lattice relaxation is calculated individually for each excited state determines whether the weak or strong particle–lattice coupling situation applies. Furthermore, we want to know how important these effects actually are.

5.2. Excited states in the self-consistently determined particle potential

The ground state couples only to lattice modes which preserve the full cubic symmetry. The same is true for non-degenerate excited states (exceptions occur in case of near degeneracy, see below). These symmetry preserving deformations, however, may be different depending on whether the light particle is in its ground state or in an excited state. In other words, the total energy of the system, with the constraint that the particle occupies a certain excited state, can be lowered compared with the value corresponding to the lattice configuration of the self-trapped ground state (see section 5.1) if the lattice undergoes a symmetry-preserving extra deformation. In the case of a degenerate excited state some symmetry-preserving extra deformation may also be present. In addition, however, coupling to Jahn–Teller active modes (see, e.g., Bersuker 1984) will lead to a further shift of the equilibrium lattice configuration of a self-trapped excited state towards configurations of lower symmetry and lower total energy. As a consequence of these effects the self-consistently determined vibrational energies E_i ($i = 1, 2 \ldots$) will be different from the E_i values given in table 2 (lines marked by STGS) and $\Delta E_i^{\min}$, E_i^{def} (lowering of the potential minimum due to self-trapping, deformation energy) will not be the same as the corresponding values calculated for the ground-state configuration.

The first excited state (state 1), which has symmetry T_{1u} and which is three-fold degenerate, may linearly couple to lattice modes transforming according to the one-dimensional representation A_{1g} (these modes possess the full cubic symmetry) as well as to Jahn–Teller active modes which transform according to two-dimensional (E_g) or three-dimensional (T_{2g}) representations of the cubic group (see Klamt 1987, Bersuker 1984). A typical case of E-mode coupling which leads to a tetragonal distortion of the octahedron is shown in figure 5.

In order to determine whether the first excited state couples predominantly to E or T modes, two calculations for each hydrogen isotope have been performed in which the wavefunction and the lattice distortion have been determined self-consistently. In the first series of calculations tetragonal symmetry of the wavefunction is required. This symmetry condition leads automatically to a tetragonal lattice distortion which is built up by lattice modes possessing the full cubic symmetry (A_{1g}) and by modes with E_g symmetry. The solution obtained by this procedure corresponds to one of the three equivalent minima (in case of dominant E-mode coupling) or saddle points (dominant T-mode coupling) of the adiabatic energy surface of the (linear) T-($e + t_2$) Jahn–Teller effect (see e.g., Bersuker 1984). In the following this kind of calculation is given the label coupling to E modes. In the second series of calculations the iteration has been started with one of the four linear combinations of the three eigenfunctions of the T_{1u} state (as obtained in the ground-state lattice configuration) which inevitably leads to a trigonal lattice distortion (see, e.g., Bersuker 1984). In this case no symmetry restrictions have been imposed on the wavefunctions.

After a few iteration steps first a self-consistent hydrogen state associated with trigonal lattice distortions is obtained. This state will be given the label T-mode coupling in the following. However, it turns out to be unstable against small symmetry-breaking perturbations, e.g., small numerical 'noise'. After many iteration steps one eventually

obtains a state with tetragonal symmetry which is identical to what is obtained in the first series of calculations (E-mode coupling).

This shows that the trigonal points of the adiabatic potentials for the lattice motion, as studied in the second series of calculations, are saddle points whereas E-mode coupling gives the stable points. Table 4 gives a comparison of the various energies which are obtained for the following situations:

(a) if the first excited state is calculated in the ground-state configuration,
(b) for coupling to E modes,
(c) for coupling to T modes.

It is seen that, in agreement with the above-mentioned stability analysis, E-mode coupling gives for all hydrogen isotopes the largest energy gain due to self-trapping.

A comparison of the total energies for situations (a) and (b) gives us the sum of the coupling energy to pure E modes and of the extra coupling to the symmetric (A_{1g}) modes (the difference to the coupling in the ground state). The same comparison for situations (a) and (c) gives the coupling energy to pure T modes plus the energy gain due to the extra coupling to A_{1g} modes. The extra coupling energies to A_{1g} modes are identical for situations (b) and (c) (at least for linear coupling). The two series of calculations (b) and (c) therefore give two equations for the three unknown coupling energies. On the other hand table 4 shows that in many instances coupling to T modes (plus A_{1g} modes) leads to an energy gain which is very small in comparison with the one obtained for E-mode coupling. In such cases a comparison of the total energies as obtained for situation (a) and (b) gives directly the energy gain due to pure E-mode coupling. In other cases the energy gain due to T ($+A_{1g}$) mode coupling is non-vanishing. For example, for the lighter particles (μ^+, π^+) the energy gain caused by E-mode coupling is quite large, of the order of 20 meV, and even T-mode coupling leads to an energy reduction by a few meV. We argue that the latter is mainly due to coupling to the symmetric mode and that the true coupling energy to E modes is thus given by the difference of the self-trapping energies for case (b) and (c) in table 4.

This conjecture can be made plausible if we look at the displacements of the nearest-neighbour atoms of the particle. Table 5 gives the displacements for E-mode coupling together with the trace of the double-force tensor, determined from the calculated ΔV and equation (12). Table 6 shows the absolute values of the displacements for T-mode coupling together with an average displacement characterizing the symmetric part of the displacement field. Obviously, both are almost identical. This supports our view that the displacements obtained in the calculations (c) being essentially of A_{1g} symmetry are equal to the symmetric part of the displacements which are obtained for E-mode coupling. The third line in table 6 shows the displacements in the ground-state configuration for comparison. The energy gain due to E-mode coupling is for the proton only 4 meV (2 meV) if pair potential II (I) is used. This means that the weak coupling case (see section 5.1) is realized. If the characteristic E mode is assumed to have a frequency $\omega_E \approx 0.5\omega_D (\hbar\omega_E \approx 14\text{meV}$ in Pd) we find a coupling constant $\lambda_E = \Delta E/\hbar\omega_E \approx 0.28(0.14)$.

The self-consistent calculation of the second and third excited state (table 7) has been performed without symmetry restrictions imposed on the lattice distortions and without chosing special start wavefunctions in the iteration. In both cases we end up with a tetragonal distortion (E-mode coupling). In the case of the second excited state with T_{2g} symmetry the interpretation, as for the first excited state, is a Jahn–Teller effect with predominant E-mode coupling. The third excited state (A_{1g}) is, however, non-degenerate and the explanation for the appearance of E-mode coupling must be a pseudo Jahn–Teller effect due to coupling to

Table 4. Vibrational energy E_1^{vib} and change of the vibrational energy ΔE_1^{vib} of the first excited state. Change of the energy of the bottom of the potential well ΔE_1^{min}, deformation energy E_1^{def}, and the total energy gain ΔE_1^{tot} due to self-trapping. (a) calculations performed in the ground-state lattice configuration (for E_1^{vib} see also table 2; for $\Delta E_1^{min} = \Delta E_0^{min}$, $E_1^{def} = E_0^{def}$ see also table 3); (b) and (c) self-consistent lattice relaxation according to the proper wavefunction—(b) coupling to E modes (c) coupling to T modes. Mesh width 0.0647Å. The values in round brackets are calculated using pair potential I, the others with pair potential II.

		E_1^{vib} (meV)	ΔE_1^{vib} (meV)	ΔE_1^{min} (meV)	E_1^{def} (meV)	ΔE_1^{tot} (meV)
μ^+	(a)	722 (686)	−93 (−131)	−71 (−229)	62 (142)	−102 (−218)
	(b)	663 (642)	−151 (−176)	−82 (−251)	106 (188)	−127 (−239)
	(c)	696 (670)	−119 (−148)	−85 (−257)	96 (182)	−108 (−223)
π^+	(a)	617 (582)	−79 (−107)	−68 (−224)	57 (135)	−91 (−196)
	(b)	568 (547)	−128 (−142)	−79 (−244)	94 (174)	−112 (−214)
	(c)	596 (569)	−100 (−120)	−81 (−249)	86 (170)	−96 (−199)
p	(a)	200 (190)	−27 (−37)	−55 (−199)	35 (105)	−47 (−131)
	(b)	189 (183)	−39 (−44)	−61 (−208)	47 (119)	−52 (−133)
	(c)	196 (188)	−31 (−39)	−62 (−209)	45 (118)	−48 (−131)
d	(a)	132 (127)	−18 (−25)	−53 (−194)	31 (100)	−40 (−119)
	(b)	125 (123)	−25 (−29)	−57 (−201)	39 (109)	−43 (−121)
	(c)	130 (126)	−21 (−26)	−57 (−201)	38 (108)	−40 (−119)
t	(a)	103 (101)	−15 (−20)	−51 (−192)	29 (98)	−36 (−114)
	(b)	99 (98)	−19 (−23)	−55 (−197)	36 (105)	−38 (−115)
	(c)	102 (100)	−16 (−21)	−55 (−198)	35 (104)	−37 (−114)

Table 5. Displacement of nearest-neighbour Pd atoms (relative to their rigid-lattice positions) for coupling of the first excited state to E modes in percent of the lattice constant ($a = 3.88$ Å). Δl^2 displacements for atoms on the tetragonal axis, Δl^1 displacements for atoms on a plane perpendicular to the tetragonal axis (see figure 1), trace of the double-force tensor. Values in brackets calculated with pair potential I, the others with pair potential II.

	$\Delta l^1/a$[%]	$\Delta l^2/a$ (%)	TrP (eV)
μ^+	0.54 (1.13)	2.46 (2.85)	9.99 (11.70)
π^+	0.53 (1.14)	2.29 (2.68)	9.63 (11.33)
p	0.49 (1.16)	1.38 (1.86)	7.81 (9.60)
d	0.49 (1.17)	1.16 (1.68)	7.39 (9.25)
t	0.49 (1.17)	1.06 (1.60)	7.19 (9.09)

nearly degenerate states.

To summarize this section, we have found that for the description of inelastic neutron scattering (INS) spectra of p, d and t in Pd the weak coupling picture has to be applied (see Klamt 1986, Stoneham 1975). This means that the excitation energies in the potential well of the fixed ground-state lattice configuration (Franck–Condon energies) do not give the correct peak positions in the neutron scattering spectra. On the other hand we find that the excitation energies to the fully relaxed excited states (position of the zero-phonon line) are very close to the Franck–Condon energies so that in practice this difference is absolutely irrelevant with regard to the peak positions. The next question is whether the

Table 6. $(\Delta l/a)_T$: Absolute values of displacements of nearest-neighbour Pd atoms (relative to their rigid lattice position) for coupling of the first excited state to T modes. $\overline{(\Delta l/a)}_E = \frac{2}{3}(\Delta l^1/a) + \frac{1}{3}(\Delta l^2/a)$ (Δl^1, Δl^2 from table 5), i.e. average displacement for E-mode coupling. $(\Delta l/a)_g$: displacements in the ground-state configuration. Values in brackets correspond to pair potential I.

	μ^+	π^+	p	d	t
$(\Delta l/a)_T$ (%)	1.24 (1.76)	1.16 (1.69)	0.80 (1.40)	0.72 (1.34)	0.68 (1.32)
$\overline{(\Delta l/a)}_E$ (%)	1.18 (1.70)	1.12 (1.65)	0.79 (1.39)	0.71 (1.34)	0.68 (1.31)
$(\Delta l/a)_g$ (%)	0.97 (1.54)	0.92 (1.50)	0.68 (1.32)	0.63 (1.29)	0.61 (1.27)

Table 7. Characteristic energies (see table 4) for the second and third excited state (E_2 and E_3 respectively) (a) ground-state lattice configuration (b) coupling to E modes. In brackets the values obtained in pair potential I are given.

		E_2^{vib} (meV)	E_2^{def} (meV)	ΔE_2^{tot} (meV)	E_3^{vib} (meV)	E_3^{def} (meV)	ΔE_3^{tot} (meV)
p	(a)	280 (263)	35 (105)	−57 (−145)	301 (281)	35 (105)	−56 (−145)
	(b)	262 (254)	57 (130)	−64 (−148)	288 (267)	60 (137)	−59 (−147)
d	(a)	185 (177)	31 (100)	−47 (−129)	198 (187)	31 (100)	−46 (−129)
	(b)	175 (172)	46 (117)	−51 (−131)	191 (179)	48 (122)	−47 (−130)
t	(a)	145 (140)	29 (98)	−42 (−122)	155 (147)	29 (98)	−41 (−122)
	(b)	138 (137)	41 (111)	−45 (−123)	150 (142)	43 (115)	−42 (−123)

quite asymmetric shape of the first INS peak in Pd (Rush *et al* 1984) may be attributed to the Jahn–Teller effect of the first excited state. In a paper by Klamt (1987) the line shape of this INS peak could be very well described assuming a Jahn–Teller effect with dominant T-mode coupling (T–t Jahn–Teller effect) and a coupling constant of about 0.26. Our calculations, however, give dominant E-mode coupling. This means that we do not have the complicated vibronic spectra of the T–t Jahn–Teller system but simply shifted potential surfaces. The coupling constant on the other hand is of the right order of magnitude 0.28 (0.14). An explanation of the asymmetric line shape in terms of a Jahn–Teller effect is, nevertheless, doubtful in our opinion.

Finally, in table 8 we compare the calculated excitation energies with the measured peak positions (information on line intensities requires the calculation of matrix elements, see Christodoulus and Gillan 1991). The experimental data are obtained for $PdH_{0.014}$ and $PdD_{0.014}$ (Rush *et al* 1984).

In former papers (Elsässer *et al* 1991b, 1992) the *ab initio* data for the hydrogen vibrations in the β-phase PdH were compared with the data obtained on $PdH_{0.014}$ (Rush *et al* 1984). A good agreement could be achieved by ascribing a small structure in the INS spectra at 115 ± 5 meV to an $e_{110}^{(3)}$ excitation. As shown in table 8, our present data as well as the *ab initio* data for Pd_4H agree better with the INS spectra if we refrain from attributing an excitation to this small structure but consider it as statistical noise, in line with the interpretation of Rush *et al* 1984 (however, not with their attribution of perturbed oscillator states without proper splitting of degeneracies due to cubic symmetry, see Elsässer *et al* 1992).

Table 8. Excitation energies to the first, second and third excited state. FC (Franck–Condon): excitation energy in the lattice configuration of the ground state, ZP (zero-phonon peak): energy difference between the excited state in the new equilibrium lattice configuration and the ground state, Exp: experimentally determined peak positions in the inelastic neutron scattering spectra. The *ab initio* results for undistorted Pd_4H at the equilibrium lattice constant (a = 3.94 Å) (Elsässer *et al* 1991b) are marked Pd_4H. Values in brackets obtained with pair potential I, the other with pair potential II.

	1 peak			2 peak			3 peak		
	FC	ZP	Exp	FC	ZP	Exp	FC	ZP	Exp
p	88	83	69.0± 0.5	168	160	137 ± 2	189	186	156 ± 3
	(81)	(78)		(155)	(150)		(172)	(169)	
	83 (Pd_4H)			158 (Pd_4H)			179 (Pd_4H)		
d	58	55	46.5± 0.5	111	107	–	124	123	–
	(54)	(52)		(104)	(101)		(113)	(112)	
	54 (Pd_4H)			104 (Pd_4H)			118 (Pd_4H)		
t	45	43	–	87	84	–	97	96	–
	(42)	(41)		(82)	(80)		(89)	(88)	
	43 (Pd_4H)			82 (Pd_4H)			93 (Pd_4H)		

6. Particle states localized at tetrahedral sites

Calculations in the periodic particle potential of the rigid Pd lattice (a = 3.88 Å), performed imposing periodic boundary conditions on the particle wavefunctions, show that for all hydrogen isotopes including the light ones (μ^+, π^+) excited states exist in which the particle is mainly localized in the vicinity of the tetrahedral site. The lowest energies of such states as calculated using pair potential I for π^+, p, d, t are shown in figure 6 together with the corresponding potential energy profile along the ⟨111⟩ direction, which is the direction joining the O and T site via the lowest saddle point S_{111}. For p, d, t the occupation probability at the T site is more than 99% (defined as the occupation probability within a sphere with a radius corresponding to the distance between the T site and S_{111}). For π^+ and μ^+ the occupation probability at the T site is still larger than 95% although the energy levels are far above the saddle point S_{111}. This is a consequence of the fact that the passage through the saddle point is very narrow and the potential rises very steeply along other directions. The narrow passage in turn leads to high costs of transverse kinetic energy in the narrow passage due to the uncertainty relation.

It is now self-suggesting to investigate self-localized T states. As usual, this is done requiring that the particle wavefunction vanishes at the surface of a sphere of sufficiently large radius around the T site. It turns out that the light particles (μ^+, π^+) do not localize completely at a T site; there is always some energy gained as the radius of the sphere is increased further and further in the calculations. Nevertheless, it can be expected that excited states of μ^+ and π^+ also exist and are localized mainly at the T site and which, furthermore, produce lattice distortions that are quite different from the ground-state lattice configuration. The energies of such states have not been determined for μ^+ and π^+, however. From table 9, which gives the corresponding energies for the heavier isotopes, it is clear that they must lie above the ground state by considerably more than 200 meV. The energies characterizing the tetrahedral state of p, d, and t in (a) the rigid lattice and (b) after self-localization are given in table 9. The energy difference between self-localized T and O states ranges from 303 (203) meV for the proton and 255 (164) meV for the triton. The values computed with pair potential I are given in brackets. We think that the

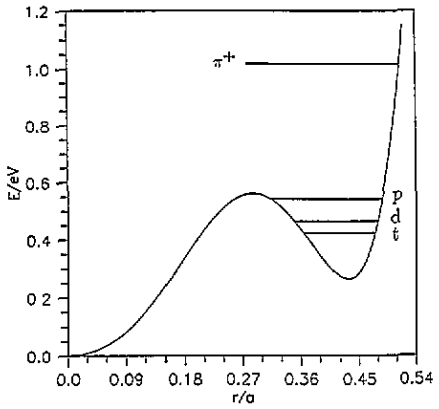

Figure 6. The lowest energies of states for π^+, p, d, t for which the particle wavefunctions in the rigid Pd lattice are mainly localized in the vicinity of the tetrahedral site, represented in the energy versus displacement curve for Pd along ⟨111⟩ (calculated with pair potential I).

calculations with pair potential II (the other values) can describe these energy differences reasonably well since this potential gives a good description of the shape of the hydrogen potential at the O site as well as at the T site in particular at the lattice constant of PdH. A good description of the potential shape at T for that lattice parameter is important because then the distance to the nearest neighbours of the T site is approximately equal to the one obtained after self-localization of hydrogen at the T site (see below). Furthermore, pair potential II reproduces the *ab initio* energy differences between the minimum of the two wells at T and O as obtained for PdH, Pd_4H (see figures 2 and 3) and at the Pd lattice constant (the *ab initio* value is approximately 320 meV (Elsässer *et al* 1992) pair potential II gives 312 meV). An uncertainty comes in through the forces on the nearest-neighbour atoms since pair potential II has a sharp bend just above the corresponding distance (see figure 4). Therefore uncertainties in the interpolation of the force obtained at distances $\sqrt{3/4}a$ ($a = 3.88$ Å) and $0.5a$ (nearest-neighbour distances at T and O in the unrelaxed Pd lattice) result in uncertainties in the forces at the relaxed positions and in the calculation of lattice relaxations. On the other hand the fact that the energy curves along ⟨111⟩ are well reproduced by $V^{II}(r)$ for different lattice parameters indicates that these uncertainties should not be serious. The nearest-neighbour atoms of p, d or t self-trapped at a T site are displaced by 1.86% (2.41%), 1.78% (2.34%) or 1.75% (2.31 %) of the lattice constant ($a = 3.88$ Å).

The energy differences between self-trapped T and O ground states are certainly too high to lead, at moderate temperatures, to a sizable equilibrium occupation of T sites by the hydrogen isotopes. However, these energies may have some relevance as they might be used to get a very crude idea about the activation energies of particle hopping via an intermediate T site.

Finally we want to discuss how significant the effects are which are introduced by the wavefunction dependence of the lattice relaxation. For this purpose calculations have been performed in which the extension of the particle wavefunction has been neglected in the determination of the lattice relaxation, i.e. in computing the forces via (6*c*) or (8) hydrogen is treated as a classical particle located at the T site. If pair potential II is used in these calculations one obtains $E^{def} = 111$meV and $\Delta E^{min} = -277$ meV and for the vibrational energies in the particle potential corresponding to the relaxed configuration created by the

Table 9. (a) Vibrational energy in the rigid Pd lattice of the lowest excited state centred at a T site (E^{vib} measured from the minimum of the potential well at the O site, E_T^{vib} measured from the potential minimum at the T site, total energy difference $E_T - E_O$ between the lowest tetrahedral state and the ground state (localized at the O site) as calculated in the rigid Pd lattice. (b) Vibrational energy E_T^{vib} (measured from the T-site minimum), change ΔE^{vib} of the vibrational energy compared with the rigid-lattice value, energy shift ΔE^{min} of the potential minimum at the T site, deformation energy E^{def} and total self-trapping energy ΔE^{tot} for that lowest-lying state which is self-trapped at the T site. Values in brackets correspond to pair potential I, the others to pair potential II. Mesh width used in calculating the particle wavefunction: 0.0647 Å. *Ab initio* results for the corresponding states in PdH at the equilibrium lattice constant (a = 4.07 Å) (Elsässer *et al* 1991b) are marked by (PdH).

		E^{vib} (meV)	E_T^{vib} (meV)	ΔE^{vib} (meV)	ΔE^{min} (meV)	E^{def} (meV)	ΔE^{tot} (meV)	$E_T - E_O$ (meV)
	(a)	606.5	294					477
		(541.2)	(277)					(410)
p			213 (Pd_4H)					
	(b)		244	−50	−308	147	−212	303
			(207)	(−70)	(−479)	(228)	(−322)	(203)
	(a)	522.2	210					437
		(459.5)	(195)					(371)
d			*150* (Pd_4H)					
	(b)		175	−35	−300	136	−199	271
			(146)	(−49)	(−467)	(214)	(−303)	(177)
	(a)	483.5	171					416
		(423.1)	(159)					(352)
t			123 (Pd_4H)					
	(b)		143	−28	−296	132	−192	255
			(119)	(−40)	(−462)	(208)	(−294)	(164)

point-like particle E_T^{vib} = 252 meV (p), E_T^{vib} = 179 meV (d), and E_T^{vib} = 146 meV (t) is found. A comparison with the corresponding entries in table 9 shows that the modifications in the vibrational energies due to the inclusion of wavefunction-dependent lattice relaxation in the calculation is only a few per cent. The effect on E^{def} or ΔE^{min} is larger but in the sum $\Delta E^{min} + E^{def}$, which enters into the energy balance, the effect is again only of this order of magnitude. The same holds for ΔE^{tot} (if calculated from the data given above one obtains −208 meV (p), −197 meV (d) and −191 meV (t) as well as for the energy difference $E_T - E_O$ between the 'ground states' at the T and O site.

7. Diffusion

A careful treatment of quantum diffusion of hydrogen isotopes within the framework of Holstein's occurrence probability approach valid above approximately half of the Debye temperature (see, e.g., Klamt and Teichler 1986a, 1986b, Emin *et al* 1979, Sugimoto and Fukai 1980) requires the calculation of a few parameters among which the most important ones are the activation energies, which are needed to create the lowest so-called coincidence configurations, and the tunnelling matrix elements. It is not the aim of the present article to perform such calculations. In particular, the computation of tunnelling matrix elements would be rather difficult because these are quite small in FCC metals. In this paper we only present the activation energies required in order to create ground-state–ground-state coincidences. To obtain these quantities, we have performed a calculation imposing the

constraint that the particle wavefunction is equally distributed among two neighbouring O sites. The values for the different hydrogen isotopes obtained with pair potential II (I) are for μ^+: 22 (66) meV, π^+: 20 (62) meV, p: 10 (48) meV, d: 9 (46) meV and t: 8 (44) meV. The values derived with pair potential II are probably somewhat too small because, as already mentioned, it gives a too small value of tr$P$. In both cases the activation energies are much smaller than the ones determined from measurements (data are available for temperatures above 130 K, for a collection of data see Fukai and Sugimoto 1985). This observation is not surprising because the tunnelling matrix elements for the ground-state coincidences and for the heavier hydrogen isotopes (p, d, t) are expected to be very small. On the other hand, such coincidences could be relevant for μ^+ and π^+.

Very crude estimates for the activation energies required to generate higher coincidences may be obtained from the excitation energies to excited states plus roughly half of the total self-trapping energies of the state considered. Clearly a more adequate treatment is required for a thorough discussion of the temperature dependence and the anomalous isotope effect found in the diffusivity of hydrogen isotopes in Pd (for a review, see Fukai and Sugimoto 1985 and 1992).

8. Conclusions

Because of the development of better computers and more efficient computer algorithms it has become possible in the past few years to calculate *ab initio* the vibrational properties of hydrogen isotopes in metals. In spite of this great step, there are two shortcomings of the available *ab initio* methods.

(i) The calculations, which are mostly based on the supercell method, are very time-consuming. As a result, only quite small supercells according to concentrated metal–hydrogen systems can be considered, whereas for many real materials, for instance Fe, the hydrogen solubility is low. Furthermore, the local structural distortion of the host lattice in the surroundings of H is mostly restricted by symmetry for small supercells, so that only the homogeneous volume relaxation due to hydrogen loading is taken into account.

(ii) The wavefunction of the hydrogen isotope is considered as point-like. In reality, however, it is extended and depends both on the isotope mass and on the particle state, which has an influence on the forces on the host atoms and on the host-atom configuration and hence in turn on the potential surface of the particles.

To cure these deficiencies, we step back from a pure *ab initio* calculation and represent the hydrogen–metal interaction by an effective pair potential which incorporates as much as possible the electronic degrees of freedom. In contrast to former work of other authors (see introduction), we thereby do not make use of experimental data (which anyway, are not available for many metals) but use almost exclusively *ab initio* data, namely the energy versus displacement curves and the forces exerted by the classical particles on the host atoms, which are calculated either directly or from the (*ab initio* determined) volume expansion upon loading of the host with hydrogen.

As an application of the theory the properties of isolated hydrogen isotopes in Pd and Fe (see part II) are calculated with special emphasis on the influence of the local lattice distortions. In summarizing the main results obtained for Pd we divide the procedure of calculating the properties of self-trapped states into two steps which could have been performed one after the other. The two steps represent different degrees of complexity.

In the first step we neglect the more delicate quantum aspects addressed in (ii) which are related to the wavefunction-dependent lattice relaxation. If this is done the first task is

to determine the displacements of the host atoms if a 'point-like' hydrogen atom is placed at a few selected interstitial sites at which the formation of self-localized particle states is likely. In Pd these are the octahedral (O) and tetrahedral (T) sites. This is within the range of *ab initio* calculations although it requires sufficiently large supercells and consequently a considerable amount of computer time. Given this fixed host lattice configuration, the potential surface for the hydrogen motion has to be determined. This is a much more demanding task which would require a large number of calculations for large supercells and to proceed in this way does not seem possible in the near future. In the present calculations the particle potential surface as well as the lattice relaxation have been determined with the help of our pair potential description of the particle–host interaction. It has been shown that in particular our pair potential II gives a very reliable description of the potential surfaces in a rigid Pd lattice and at several lattice constants for all energies which are relevant to the calculation of equilibrium properties. The advantage of pair potential I lies in the better description of the particle potential at higher energies which might become relevant in molecular-dynamics simulations.

In the calculation of lattice relaxation it is essential that the pair potential gives reliable values for the forces exerted on neighbouring host atoms at the distances which become relevant at the relaxed configuration. As shown in the text, pair potential II seems to comply with these requirements very well. In the particle potential which is constructed as discussed above and which is held fixed independent of the mass of the hydrogen isotope or of the excitation state, the vibrational states of the various hydrogen isotopes are then to be determined. As discussed below, some of the quantities of interest are already very well reproduced in Pd by a calculation of this type. We therefore suggest an even more simplified version leading to essentially identical results, which might be carried out completely *ab initio*. In this simplified version the relaxed lattice configuration if hydrogen is placed at one of the selected sites has to be determined, whether *ab initio* or using a hydrogen–host pair potential, but instead of determining the hydrogen potential surface at this locally relaxed configuration the potential surface may be constructed for a homogeneously deformed host lattice which is chosen in such a way that the distances to the nearest-neighbour host atoms agree with the ones obtained in the locally relaxed configuration. In some cases the next-nearest-neighbour distances have to be adjusted as well which might require a reduction of the symmetry of the host lattice. We come to this point in part II of the paper (Krimmel *et al* 1994). Since it is absolutely essential to take into account the lattice relaxation properly this is the minimum effort which is to be made in order to get meaningful results. The argument in favour of the simplified procedure comes from a comparison of the hydrogen vibrational energies in Pd as determined by the present calculation for the locally relaxed configuration with the results obtained from *ab initio* calculations on small supercells and at lattice parameters fulfilling the above mentioned requirements (Elsässer *et al* 1991a, 1991b).

The next step in the calculation has to include the dependence of the lattice relaxation on the particle wavefunction which in turn depends on the isotopic mass and on the vibrational state. This step is clearly out of the range of *ab initio* calculations. It turns out that if full account of the finite extension of the wavefunction is made, the vibrational energies of p, d, t change only slightly from the values which are calculated if the particle potential is held fixed and is taken as that obtained for a self-trapped 'point-like' particle. For p, d, t the changes are typically of the order of several meV or several % with a tendency to increase as one goes to higher excited states. They become also larger for the light isotopes π^+, μ^+. An explicit comparison along these lines has been given in section 6 for the lowest vibrational state localized at a T site, implicit information in this respect on the states localized at O sites

is contained, for example, in the tables comparing E-mode with T-mode coupling and with energy levels determined in the ground-state configuration. Similarly the energy differences between the 'ground states' of the various hydrogen isotopes once self-trapped at T and once at O sites are very well recovered if the wavefunction dependence of lattice relaxation is entirely neglected. The influence of the wavefunction in this case is indeed particularly small due to a partial cancellation of effects. For instance, the sum of deformation energy and of the reduction in potential energy (lowering of the potential minima at T and O) associated with self-trapping are nearly independent of the particle mass, whereas the dependence of the individual terms is significant.

On the other hand quantities like the displacements of nearest-neighbour atoms or the double-force tensor P are strongly influenced by the extension of the particle wavefunction, in particular if the light isotopes π^+, μ^+ are included in the consideration. The isotope effect in these quantities is entirely due to the extension of the particle wavefunction. The same is true for the Jahn–Teller coupling energies of excited states as well as for the resulting anisotropy of the lattice displacements and of the double-force tensor in the static Jahn–Teller distorted configurations. The Jahn–Teller coupling has been determined to be dominant in lattice modes with E-symmetry with a coupling energy of a few meV (for p, d, t). The Jahn–Teller effect might be relevant to the interpretation of line shapes of inelastic neutron scattering spectra and might also become visible at elevated temperatures and in anisotropically strained samples.

Pair potentials describing the hydrogen–metal interaction which are constructed along the lines given in the present paper not only prove useful in the calculation of equilibrium properties of diluted metal–hydrogen systems but also provide a solid basis for the calculation of transport properties. In this respect they can be used either in order to calculate some basic quantities which enter into current theories of quantum diffusion (see section 7) or in quantum or classical molecular dynamic simulations. In both cases a large number of configurations has to be explored and *ab initio* methods can so far be employed only for refinements at a few particular configurations.

Acknowledgements

The authors are indebted to C T Chan, K M Ho and A Klamt for helpful discussions.

References

Bersuker I B 1984 *The Jahn–Teller Effect and Vibronic Interactions in Modern Chemistry* (New York: Plenum)
Burns G 1977 *Introduction to Group Theory with Applications* (London: Academic Press)
Christensen O B, Stoltze P, Jacobsen K W and Nørskov J K 1990 *Phys. Rev.* B **41** 12413
Christodoulos F and Gillan M J 1991 *J. Phys.: Condens. Matter* **3** 9429
Elsässer C 1990 *PhD Thesis* Universität Stuttgart
Elsässer C, Fähnle M, Ho K M and Chan C T 1991a *Physica* B **172** 217
Elsässer C, Ho K M, Chan C T and Fähnle M 1991b *Phys. Rev.* B **44** 10377
Elsässer C, Ho K M , Chan C T and Fähnle M 1992 *J. Phys.: Condens. Matter* **4** 5207
Elsässer C, Zhu J, Louie S G, Chan C T and Fähnle M 1994a unpublished
Elsässer C, Fähnle M, Schimmele L, Chan C T and Ho K M 1994b *Phys. Rev.* B submitted
Elsässer C, Fähnle M, Chan C T and Ho K M 1994c *Phys. Rev.* B
Emin D, Baskes M J and Wilson W D 1979 *Phys. Rev. Lett.* **42** 791
Engberg U, Li Y and Wahnström G 1993 *J. Phys.: Condens. Matter* **5** 5543
Feynman R P 1939 *Phys. Rev.* **56** 340
Fukai Y and Sugimoto H 1985 *Adv. Phys.* **34** 263
Fukai Y and Sugimoto H 1992 *Defect and Diffusion Forum* **83** 87

Hayashi Y, Hagi H and Tahara A 1989 *Z. Phys. Chem.* NF **164** 815
Hellmann H 1937 *Einführung in die Quantenchemie* (Leipzig: Denticke)
Kimball G E and Shortley G H 1934 *Phys. Rev.* **45** 815
Klamt A and Teichler H 1986a *Phys. Status Solidi* b **134** 103
Klamt A and Teichler H 1986b *Phys. Status Solidi* b **134** 533
Klamt A 1986 *J. Phys. F: Met. Phys.* **16** L1
Klamt A 1987 *J. Phys. F: Met. Phys.* **17** 47
Krimmel H, Schimmele L, Elsässer C and Fähnle M 1994 *J. Phys.: Condens. Matter* **6** 7705
Leibfried G and Breuer N 1978 *Point Defects in Metals (Springer Tracts in Modern Physics 81)* (Berlin: Springer)
MacGillivray I R and Sholl C A 1983 *J. Phys. F: Met. Phys.* **13** 23
Peisl H 1978 *Hydrogen in Metals I (Topics in Applied Physics 28)* ed G Alefeld and J Völkl (Berlin: Springer) ch 3
Puska M J and Nieminen R M 1984 *Phys. Rev.* B **29** 5382
Rush J J, Rowe J M and Richter D 1984 *Z. Phys.* B **55** 283
Stoneham A M 1975 *Theory of Defects in Solids* (Oxford: Clarendon) ch 10
Sugimoto H and Fukai Y 1980 *Phys. Rev.* B **22** 670
Sugimoto H and Fukai Y 1981 *J. Phys. Soc. Japan* **50** 3709
Teichler H 1978 *Phys. Lett.* A **67** 313
Tewary V K 1973 *Adv. Phys.* **22** 757